Electrical breakdown at low pressure for planar microelectromechanical systems with 10- to 500-μm gaps

Patrick Carazzetti
Herbert R. Shea
Ecole Polytechnique Fédérale de Lausanne
Microsystems for Space Technologies Laboratory
Rue Jaquet Droz 1
CP 526
CH-2002 Neuchâtel, Switzerland
E-mail: herbert.shea@epfl.ch

Abstract. An experimental study of the dc breakdown voltage for planar MEMS interdigitated aluminum electrodes with gaps ranging from 10 to 500 μm is presented. Unlike most research on the breakdown in MEMS electrodes that was performed at atmospheric pressure, this work focuses on the effect of gas pressure and gas type on breakdown voltage, because this is central for chip-scale plasma generation and for reliable operation in aerospace applications. The breakdown voltage is measured in helium, argon, and nitrogen atmospheres for pressures between 10^2 to 8.10^4 Pa (1 to 800 mbar). For higher values of the pressure P, or of the gap d (i.e., for high values of the Paschen reduced variable $P_{red}=P\cdot d$), classical Paschen scaling is observed. For lower values of P_{red}, however, significant deviations are seen: the V_{bd} versus. Pd curve shows an extended flat region rather than a narrow dip. These differences cannot be attributed to field emission, but are due to the many length scales effectively present in a planar geometry (on-chip and even off-chip) that leads to the superposition of several Paschen curves. Guidelines are formulated for low-pressure operation of MEMS to avoid or encourage breakdown. [DOI: 10.1117/1.3152368]

Subject terms: Paschen curve; breakdown voltage; microelectromechanical systems; planar interdigitated electrodes; aluminum; helium; argon; nitrogen; mean free path.

Paper 08159SSR received Oct. 14, 2008; revised manuscript received Feb. 17, 2009; accepted for publication Feb. 23, 2009; published online Jul. 2, 2009. This paper is a revision of a paper presented at the SPIE conference on Reliability, Packaging, Testing, and Characterization of MEMS/MOEMS VII, January 2008, San Jose, California. The paper presented there appears (unrefereed) in SPIE Proceedings Vol. 6884.

1 Introduction

1.1 *Paschen Curves in Microelectromechanical Devices*

Most of the research on Paschen curves applied to microelectromechanical system (MEMS) devices, i.e., to micron-size gaps, has focused on understanding safe operating conditions to design electrostatic actuators operating at high voltages (of the order 200 V) with gaps between electrodes of orders of a micron or even less. The limitation of the Paschen curve at micron-scale gaps at atmospheric pressure has become clear in the past few years.[1–6] The importance of the role of field emission and vapor arc have been demonstrated for gaps smaller than 10 μm, leading to the description of the "modified" Paschen curve.[4] The general conclusion has been that a maximum safe voltage is 300 V for gaps 4 μm or larger at a pressure of one atmosphere, and that the breakdown voltage decreases rapidly for smaller gaps due to field emission.[4]

One can distinguish several types of breakdowns between two conductors[7] due to: 1. stressing of the electrode surface (also known as vacuum breakdown, related to vaporization of the electrode), 2. insulator breakdown (internal or external flashover), and 3. via the gas path (Paschen). We focus in this work on the Paschen breakdown regime, since it is most relevant for MEMS devices except under very high vacuum or for gaps smaller than 5 μm.

In 1889, Paschen published a paper[8] that laid out what has become known as Paschen's law. The law expresses the breakdown voltage V_{bd} of a dielectric gas as a function of the reduced variable $P_{red}=P\cdot d$, where P is the pressure and d is the gap [Fig. 1(a)]. His work was developed to understand the breakdown voltage between large metal plates at low pressure with macroscopic gaps.

Later work by Townsend[9] led to the understanding that the breakdown is an avalanche effect caused principally by the ionization of gas molecules by electrons accelerated by the electric field. If the electron gains sufficient energy between collisions to ionize gas atoms or gas molecules, then each collision gives rise to two electrons and an ion, allowing an avalanche effect eventually resulting in a spark. This avalanche can only occur when there are sufficient gas molecules between the electrodes, i.e., if the mean free path between collisions λ is much smaller than the distance d

1932-5150/2009/$25.00 © 2009 SPIE

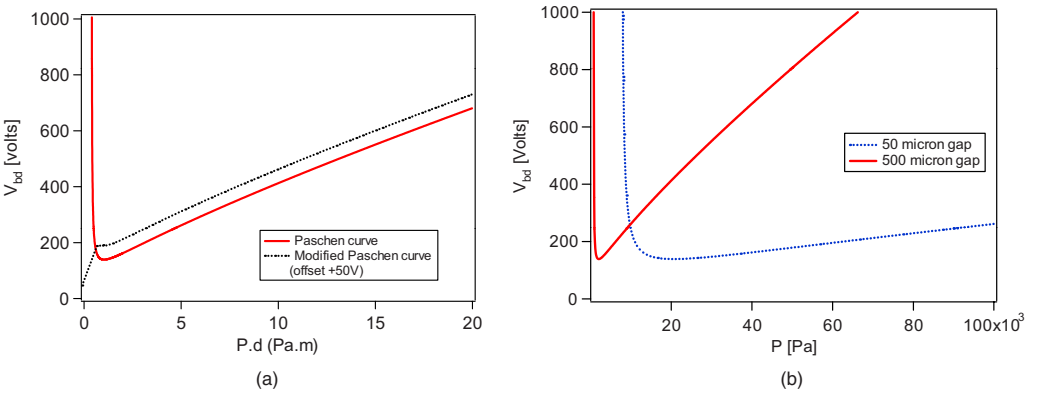

Fig. 1 (a) Paschen curve for argon plotting V_{bd} versus $P \cdot d$, showing the classical increase in breakdown voltage at large and small values of $P \cdot d$ (solid line), and the modified Paschen curve showing the drop to zero of V_{bd} as the gap goes to zero (dotted line, offset by 50 V for clarity), after Ref. 4. (b) Paschen curve in argon for a 50-μm gap (dotted line) and 500-μm gap (solid line): the minimum voltage for breakdown is the same in both cases, but the pressure at which the minimum in V_{bd} occurs is gap dependent.

between electrodes: when $\lambda \ll d$. If the pressure is too low or if the gap is too small, the avalanche breakdown (Townsend theory) cannot take place.

This absence of atoms or molecules is what gives the minimum in the Paschen curve. At large gaps or pressures, a linear relation breakdown voltage and electrode gap are found (reflecting the constant breakdown electric field of the gas), while at very small gaps one has a "vacuum isolation," where there are not enough gas atoms or molecules for the avalanche to occur. Another way to look at the breakdown is to consider the mean free path $\lambda_{electron}$ of an electron in the direction of the applied field. $\lambda_{electron}$, like λ, scales inversely with the pressure (neglecting the Ramsauer effect),[7] and so the product $P_{red}=P \cdot d$ is proportional to $d/\lambda_{electron}$, giving an indication of the number of collisions an electron undergoes when crossing the gap. The breakdown voltage V_{bd} then simply depends on the $P \cdot d$ product, with all parameters except gap and pressure being fixed.

Later work led to the understanding that the Paschen curve also depends on secondary electrons emitted from the negative electrode when impacted by the positive ions. These electrons further accelerate the breakdown process. The secondary electron yield γ depends on the cathode material.[10,11] The Paschen curve can be obtained by computing the voltage required for the process of electron emission and multiplication to become self-sustaining.[12] One obtains:

$$V_{bd} = \frac{B \cdot P \cdot d}{\ln(A \cdot P \cdot d) - \ln\left[\ln\left(1 + \frac{1}{\gamma}\right)\right]}, \quad (1)$$

where A and B are properties of the gas, and γ is a property of the electrode material.

The Paschen curves were developed for macroscopic electrodes at operating pressures from a few Pa to one atmosphere. The generality of the scaling of V_{bd} with P_{red} led researchers to apply it to MEMS devices operating in a variety of gases at one atmosphere, for which a minimum breakdown voltage of order 380 V is predicted at a spacing of 8 μm (the exact numbers depend on the gas).

As reported in Refs. 1, 2, 5, and 6 when the gaps are less than 10 μm for micromachined structures operated at one atmosphere ($P_{red} < 1$ Pa·m), important deviations are seen from the Paschen curve. This regime is one where the mean free path is of the order of the gap, thus where the Townsend breakdown cannot occur. Other types of breakdown are possible, however. As presented for instance in Refs. 4 and in 6, field emission can become important at gaps of the order of 5 μm, leading to a modified Paschen curve, which agrees with the standard Paschen curves at gaps larger than 10 μm ($P_{red} > 1$ Pa·m), exhibits a plateau of constant V_{bd} between 4 and 10 μm, and a linear drop in V_{bd} at lower gaps [dotted line in Fig. 1(a)]. Field emission can lead to local heating at microasperities on the surface of the cathode, which in turn facilitates field evaporation of the cathode, leading to a cloud of atoms and ions in which an avalanche breakdown process can start.[13]

In addition to the nature of the gas [reflected in the constants A and B of Eq. (1)] and the nature of the electrode (in the form of parameter γ), relevant parameters that must be taken into account are the mean free path of gas atom species, the surface roughness (which has a strong influence on the field emission), work function of the electrode, and the overall geometry of the electrodes, especially for planar geometries as found in MEMS and integrated circuits, which do not match the conditions of uniform electric field for which the Paschen curves were developed.

1.2 *Motivation of the Research*

With the exception of the work of one group,[12,14,15] Paschen curves for micron-scale gaps have been measured at atmospheric pressure,[1,4,16,17] typically in air, which is reasonable given that this is the normal operating condition for MEMS devices. Although Baars-Hibbe et al.[11] report on measurements down to 10 kPa, their main objective was creating atmospheric plasmas.

The main motivation for this work is to develop a chip-scale hermetically sealed plasma light source consisting of Al electrodes spaced by 10 to 500 μm sealed in a stack of three anodically bonded glass wafers. We reported on the fabrication process and optical spectra obtained from this

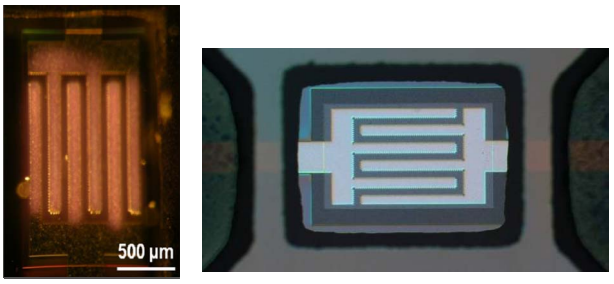

(a) (b)

Fig. 2 (a) Top view of rf plasma ignited in argon using the same electrodes used for the breakdown voltage study presented here. Details on rf operation can be found in Ref. 19. (b) Top view electrodes bonded to a patterned Pyrex chip as part of a hermetic sealing procedure.

light source in Refs. 18 and 19 for different gases and pressures. Applications for such a light source include optical pumping in chip-scale atomic clocks, leak detection, and outgassing characterization. Figure 2(a) is an optical micrograph of an rf plasma ignited in argon for the same microfabricated electrodes used for the study reported here.

To ignite the plasma discharge, a sufficient ac or dc potential ($\sim$300 V) must be applied between the electrodes. For lifetime and power consumption reasons, our chip-scale light source is operated as an rf plasma at frequencies near 20 MHz. rf operation minimizes erosion of the cathode (thus increasing lifetime), and can reduce the minimum voltage required for ignition as reported in Ref. 15.

The goal of the study reported here is to compare different electrode gap sizes and gap geometries to determine the conditions under which a plasma can be ignited with the lowest possible voltage over a wide pressure range (i.e., 10^2 to $8\cdot10^4$ Pa, or 1 to 800 mbar). rf plasmas are more complex to understand than dc plasma, with additional length scales that need to be considered, primarily because the electrons are confined by field oscillations, and the space-charge sheaths at the plasma boundary.

We therefore investigated the dc Paschen curve of the structure described in the following section, varying both the gap (from 10 to 500 μm) and the pressure (10^2 to $8\cdot10^4$ Pa) for He, Ar, and N_2 atmospheres. Our samples thus cover a very large range of P_{red}: more than 4 orders of magnitude from $P_{red}=10^{-3}$ Pa·m to 40 Pa·m, covering regimes of small P_{red} not accessible to devices (regardless of size) operated at atmospheric pressure because of the field emission occurring at small gaps.

Section 2 presents the sample design and fabrication. In Sec. 3 the measurement setup is described, and data are presented on the breakdown voltage as a function of pressure, gas type, and gap size. The experimental data are discussed in Sec. 4.

2 Sample Design and Fabrication

Interdigitated electrodes with three pairs of fingers covering 2 orders of magnitude of gap spacing were designed and fabricated. Figure 3(a) is a CAD plot showing the device layout in micrometers. Each finger is 2820 μm long and 240 μm wide. Corrugated edges were used to locally enhance the electric field and hence to lower the voltage required for breakdown. The distance separating the tip of opposite protruding patterns, shown by the scale bars in Fig. 3(b), is referred to in following text as the electrode gap spacing d. Varying only the parameter d, eight different electrode versions were designed, namely $d=10$, 20, 40, 100, 150, 200, 300, and 500 μm.

Key features of the fabrication process are the use of thick Al films deposited on insulating substrates (fused silica) and patterned with a highly anisotropic dry-etching process that avoids mask undercutting, thereby preserving the sharpness of corrugated electrode edges.

In a first step, 8 μm of aluminum were sputter deposited from a pure Al target on 100-mm fused silica substrates. The sputtering process was realized at room temperature with a dc power of 2 kW, leading to a deposition rate of 400 nm/min. The equipment used was a Spider-600 from Pfeiffer Vacuum (Nashua, New Hampshire). Next, a 10-μm-thick layer of Clariant's AZ9260 photoresist was spun and photographically defined into the mask for patterning the electrodes. Al etching was done with an inductively coupled plasma (ICP) process based on a mixed Cl_2/BCl_3 chemistry on a STS Multiplex ICP etching tool. The Al was etched at a rate of approximately 300 nm/min, and the selectivity toward the mask, considering a load of about 80% of the wafer surface, was observed to be close to unity. Figure 4(a) is an optical micrograph of a fabricated device with an electrode gap of 40 μm, whereas Fig. 4(b)

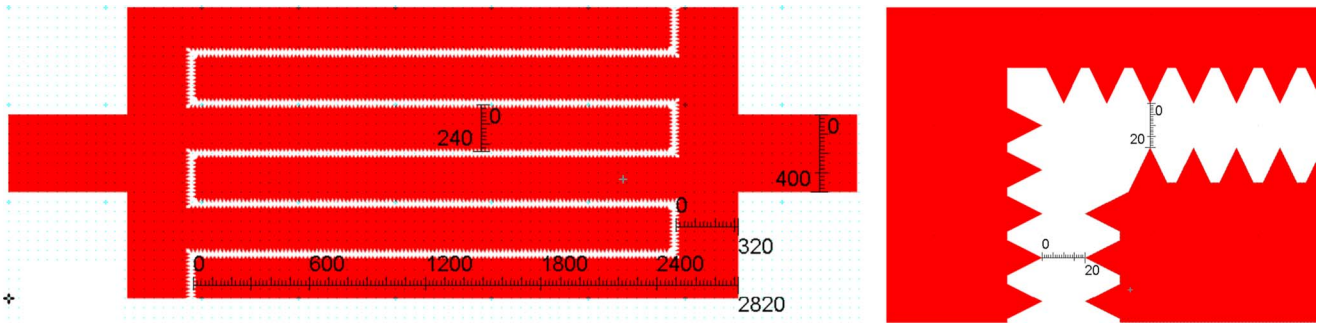

(a) (b)

Fig. 3 (a) CAD layout showing the overall footprint of a device. (b) Close-up showing the 20-μm gap separation between opposite protruding patterns. All dimensions are in micrometers.

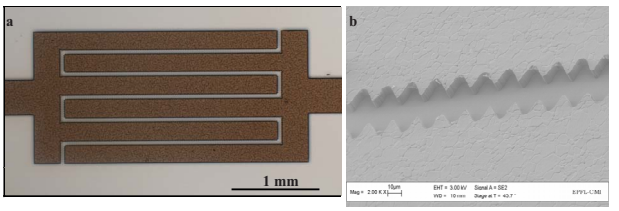

Fig. 4 (a) Optical image of a fabricated device with a gap spacing of 40 μm. (b) SEM close-up of 8-μm-thick dry-etched Al electrodes with corrugated edges.

is a SEM close-up of the patterned aluminum electrodes with smooth and vertical walls enabled by the ICP process.

3 Experimental Setup and Results

3.1 *Experimental Setup*

The dc breakdown characterization presented in this study was performed in a small vacuum chamber (volume of 0.7 l) with feedthroughs for electrical connections (MHV), pressure sensors, gas inlet, pumping, and venting [see Fig. 5(a)]. Prior to each measurement series, the chamber was pumped down to a pressure of 0.5 Pa, then purged and filled with He, Ar, or N_2. The microfabricated chips were mounted on a custom printed circuit board (PCB) with pads for wirebonds and interface to electrical contacts from the MHV feedthrough, as shown in Figs. 5(b) and 5(c), respectively.

Breakdown tests were performed by measuring the current versus voltage (I-V) characteristic of the device under test (DUT). Voltage was applied across each terminal of the DUT with a high voltage power supply (PS350 from Stanford Research Systems, Incorporated, Sunnyvale, California). controlled by a LabView program. The voltage was increased in steps of 1 V every 500 ms from an initial value of 50 V until the current increased sharply and exceeded a preset threshold value. The voltage corresponding to the sharp current rise was taken as the breakdown potential V_{bd}.[4,5] Depending on the pressure and electrode gap, the sharp rise in current was accompanied by a visible breakdown event, ranging from a weak glow covering the whole device footprint to a localized spark or glow. The compliance current was set at a sufficiently low threshold (0.05 mA) to avoid rapid destruction of the electrodes due to arcing. Paschen curves were thus plotted based on the recorded values of breakdown voltage V_{bd} versus $P \cdot d$ for pressure ranging from 10^2 to $8 \cdot 10^4$ Pa.

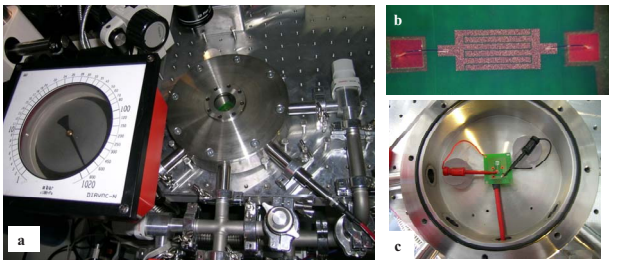

Fig. 5 (a) Vacuum chamber used for the breakdown measurements, (b) device under test (DUT), the microfabricated chip (transparent except for the Al electrode) wirebonded to the PCB, and (c) electrical contacts to the PCB.

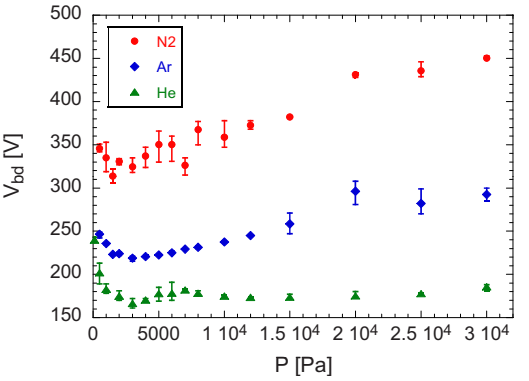

Fig. 6 Breakdown voltage V_{bd} versus pressure P measured in different gas atmospheres (He, Ar, and N_2) on three devices with 100-μm gap separation.

3.2 *Effect of the Gas Type*

To introduce the Paschen curve data, it is helpful to start with an overview of the different types of behavior that were observed. Figure 6 is a plot of breakdown voltage V_{bd} versus pressure p for three samples with an identical 100-μm gap in N_2, Ar, and He. For each pressure, the measurement was repeated five times. Solid symbols on the curves in Fig. 6 represent the average of these measurements, whereas the error bars indicate lowest and highest values of the breakdown voltage.

At first glance, typical Paschen behavior is observed, as in Fig. 1, with the minimum voltage for breakdown being lowest for He and highest for N_2.[10,17] However, a more quantitative comparison of our experimental data with published values is difficult, since V_{bd} strongly depends on the cathode material,[10,20,21] on the surface roughness,[5,21,22] and also on whether the breakdown is created in dc or rf mode.[12,15,23] It is reported that rf discharges exhibit significantly lower values of V_{bd} than dc discharges.[14] The overall shape is as expected from the Paschen theory. However, as discussed later in Sec. 3.6, this theory provides a poor fit when applied to the full pressure range, but provides a very good fit for higher $P \cdot d$ values.

One important point to notice is the double dip in the He curve, which can be clearly attributed to the different lengths of scales present in the measurement setup. The dip at 3 kPa corresponds to breakdown on the printed circuit board (gaps between wirebonds of order 3.5 mm), while the higher pressure dip (>10 kPa) is due to breakdown across the microfabricated electrodes. This important element is discussed in more detail in Sec. 3.3. The crossover from the chip-dominated regime to PCB-dominated behavior depends on electrode spacing and on gas type: it is easily visible in He, less noticeable in Ar and not observable in N_2.

3.3 *Effect of the Gap Spacing in Helium*

The crossover is clearly illustrated in Fig. 7, where experimental V_{bd} versus p curves are plotted in He for a sample

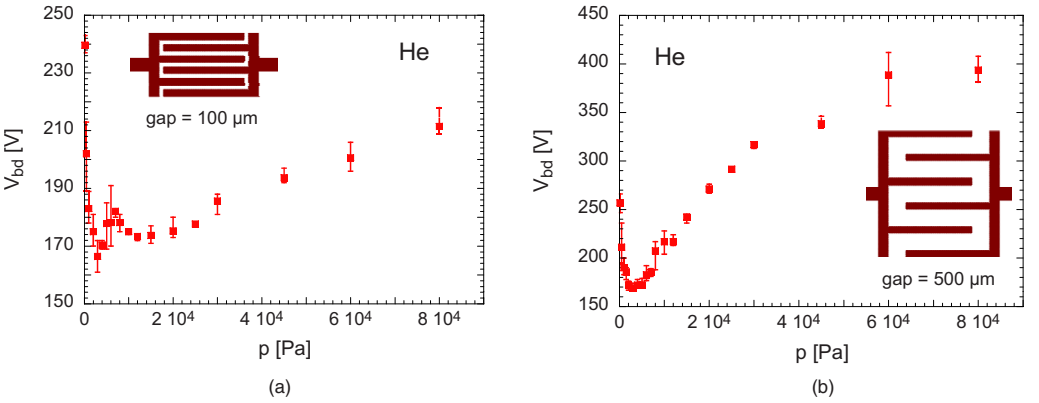

Fig. 7 Breakdown voltage V_{bd} versus pressure P measured in helium on a device (a) with 100-μm gap and (b) with a 500-μm gap.

with a 100-μm gap [Fig. 7(a)] and a 500-μm gap [Fig. 7(b)]. As illustrated in Fig. 1(b), the pressure corresponding to the minimum V_{bd} scales as $1/d$ in the Paschen model. Both devices exhibit a minimum breakdown voltage of 160 to 170 V between 2 to 4 kPa due to the PCB, as discussed in the previous section. In addition, the device with a 100-μm gap has a second dip of value 175 V located around 15 kPa, corresponding to $P \cdot d = 1.5$ Pa·m. Published data for minimum breakdown in He reported $V_{bd} = 240$ V for $p \cdot d = 5.5$ Pa·m,[20] and $V_{bd} = 150$ V for $P \cdot d = 5.33$ Pa·m (or 4 torr·cm).[17] In Fig. 8, V_{bd} data for electrode gaps from 10 to 500 μm are overlaid and plotted as a function of pressure [Fig. 8(a)] and $P_{red} = P \cdot d$ [Fig. 8(b)]. For clarity, error bars are no longer displayed. All samples except the bare PCB and the chip with the largest gap ($d = 500$ μm), exhibit a dip with minimum V_{bd} between 170 and 210 V. A correlation of these values of minimum V_{bd} with the gap spacing cannot be found.

3.4 *Effect of the Gap Spacing in Argon*

The data for breakdown in argon are presented in this section. Fig. 9 is the equivalent of Fig. 8 but for Ar (same gaps and pressures as for He). Similar behavior to He is seen, but the $P \cdot d$ range where the curves overlap is larger. The crossover from non-Paschen to Paschen behavior occurs near 1 Pa·m. For small gaps, the contributions from the PCB and from the chip are still clearly distinguishable. All the samples, except the bare PCB and the chip with largest gap ($d = 500$ μm), exhibit a dip with minimum V_{bd} between 210 and 250 V. Again, there is no correlation between these values of V_{bd} minimum and the gap spacing.

3.5 *Effect of the Gap Spacing in Nitrogen*

The data for breakdown in nitrogen are presented in this section. Fig. 10 is the equivalent of Figs. 8 and 9. Less data is available for N_2 than for Ar or He (fewer gaps sizes, same pressure range). The dips in the curves are much less marked or no longer present. For nitrogen, which is one of the gases with the highest breakdown voltages, the effect of the PCB is not visible in our data (as it would occur at lower pressures than what we used, i.e., below 100 Pa, 1 mbar). The plots fit the overall Paschen shape well, and are well represented by the reduced variable $P \cdot d$. All the measured samples exhibit minimum V_{bd} between 280 and 325 V. As expected, these values are higher than for He and Ar.

4 Discussion

The V_{bd} versus $P \cdot d$ data for He, Ar, and N_2 presented earlier in Figs 8(b), 9(b), and 10(b) are plotted using one symbol per gap spacing, reflecting how the data were acquired, i.e., by varying the pressure for a fixed gap, then moving to

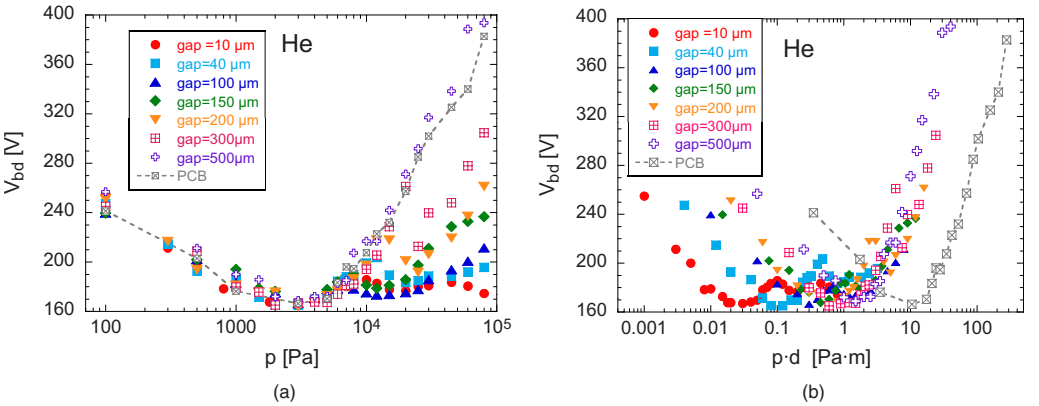

Fig. 8 (a) Breakdown voltage V_{bd} versus pressure P and (b) V_{bd} versus the product $P \cdot d$ measured in He on devices with gap spacing ranging from 10 to 500 μm. The measured curves for the bare PCB are represented by a dashed line in both graphs.

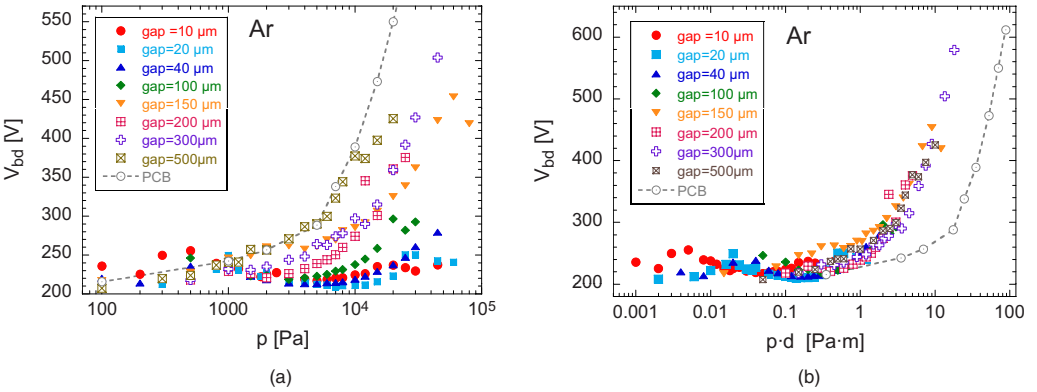

Fig. 9 (a) Breakdown voltage V_{bd} versus pressure P, and (b) V_{bd} versus the product $p \cdot d$ measured in Ar on devices with gap spacing ranging from 10 up to 500 μm. The measured curves of the PCB are represented by a dashed line.

a sample with a different gap. This same dataset can instead be plotted visually, grouping points taken at a given pressure on samples with different gaps, thus emphasizing the scaling with gap rather than the scaling with pressure. This is shown in Figs. 11(a)–11(c), where only the higher pressure values were kept. This in essence amounts to a zoom on the higher P_{red} parts of Figs. 8(b), 9(b), and 10(b).

The reduced Paschen variable P_{red} provides a very good description of the breakdown process for $P \cdot d > 1$ in view of how the V_{bd} versus $P \cdot d$ data points for different pressures and for gaps from 10 to 500 μm collapse into a single line for each gas in Figs. 11(a)–11(c). However, the Paschen theory fits the data well only for the higher Pd part of Figs. 11(a)–11(c). the solid line is a fit to the Paschen formula [Eq. (1)]. The extracted parameter B from the fit is given in Table 1. The fitted B is close to the values reported in the literature for a much more ideal geometry,[23] although the planar geometry of our electrodes present a different field distribution.

If one uses the literature values,[23] for the Paschen parameters of Ar, one finds very good agreement at high pressures in the linear regime, but at low pressures the Paschen theory predicts slightly lower V_{bd} than observed, by about 50 V.

The behavior of the samples can be divided into two regimes: high P_{red}, where classical Paschen behavior is observed, and low P_{red}, where deviations are seen. A crossover P_{red}^{thresh} can be identified, delimiting these two regimes. For helium, argon, and nitrogen, we have approximately P_{ref}^{thresh}=5, 3, and 2 Pa·m, which can also be expressed as a threshold pressure for a fixed gap. The transition occurs at lower pressures for He [Fig. 8(a)] than for Ar [Fig. 9(a)] and N_2 [Fig. 10(a)]. Almost all our data for nitrogen display standard Paschen scaling.

The divergence at lower pressure has been noted for rf discharges in Ref. 16, and field emission was proposed as a mechanism. Since our gaps can be as large as 500 μm, field emission cannot explain the observed behavior. There are two factors that might explain our data: 1. the mean free path, and 2. the planar geometry.

Figure 12 plots the approximate mean free path versus pressure for our three gases. The mean free path scales as $1/P$, and one can write:

$$\lambda \cdot P = \frac{R \cdot T}{\sqrt{2} \cdot d_{\text{atom}}^2 \cdot N_{\text{Av}}}, \tag{2}$$

where N_{Av} is Avogadro's number, d_{atom} is the effective diameter of the gas atom or molecule, T is the temperature, and R is the universal gas constant. At 293 K and using literature values for effective atom/molecule diameters, the

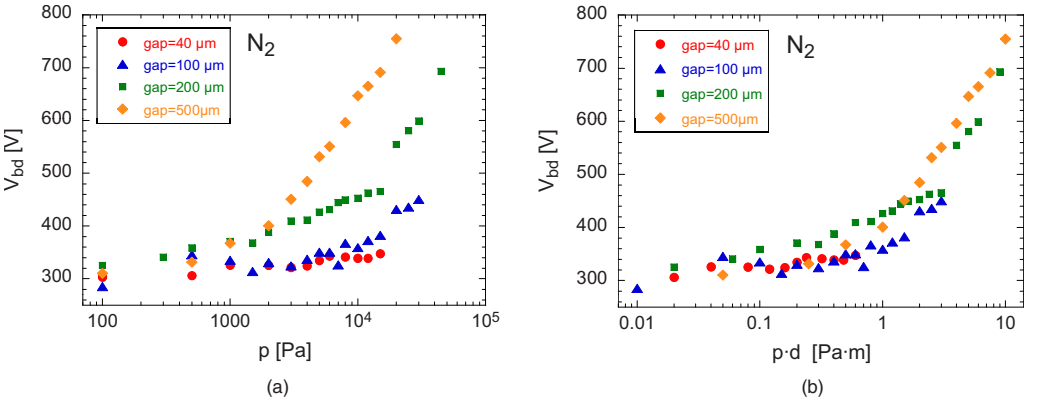

Fig. 10 (a) Breakdown voltage V_{bd} versus pressure p and (b) V_{bd} versus the product $p \cdot d$ measured in N_2 on devices with gap spacing ranging from 10 up to 500 μm.

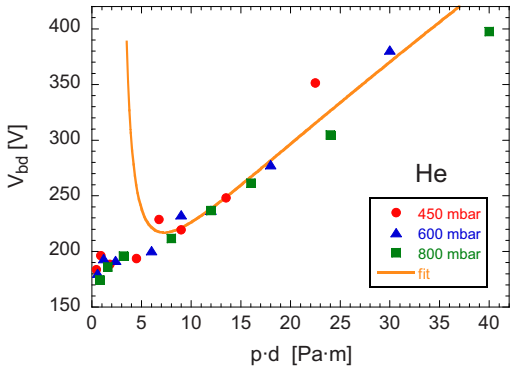

(a)

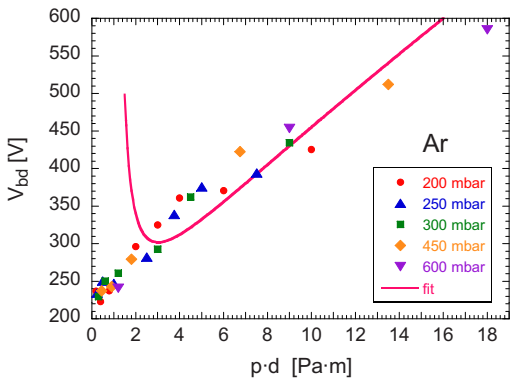

(b)

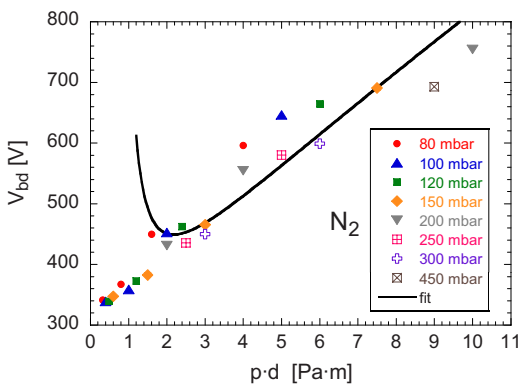

(c)

Fig. 11 Paschen curves: (a) in helium, (b) in argon, and (c) in nitrogen. Symbols correspond to experimental V_{bd} data for different gap spacings grouped by pressure rather than by gap. Lines are fits to the Paschen theory, using only the points at higher $P \cdot d$ products for fitting.

$\lambda \cdot P$ constants for He, Ar, and N_2 from Eq. (2) are: 0.02, 0.007, and 0.007 Pa·m. Recall from Sec. 1 that to have classical avalanche breakdown, one must have $\lambda \gg d$. Multiplied by 500 (corresponding to requiring $\lambda > 500 \cdot d$), one comes close to the observed P_{red}^{thresh} values.

When measuring the breakdown between two parallel plates for which the gap is much smaller than the plate size, the only relevant length scale is the gap, providing that minor precautions are taken at the plate edges. However, for a planar geometry, as is typical for MEMS devices, microelectronics, and in the test structures used here, many

Table 1 Values of B [Eq. (1)] from the literature[23] and from fits to experimental data in Figs. 11(a)–11(c).

Gas	B, values at dc from literature [V·Pa^{-1}·m^{-1}]	B, determined by fitting [V·Pa^{-1}·m^{-1}]	$\Delta B/B_{dc}$ [%]
He	26	29.83	+14.7%
Ar	135	100.04	−25.9%
N_2	256	206.2	−19.4%

length scales are present, as shown schematically in Fig. 13. With a gap of 500 μm and electrodes 8 μm thick, our situation is far from parallel plates.

Having many length scales means that one effectively superposed many Paschen curves (corresponding to the different gap lengths), from the longest to the shortest length scale, as shown in Fig. 14. The smallest length scale is the microfabricated gap, the largest of the order of the chip or PCB size. The measured Paschen curve will then be the minimum envelope of all possible Paschen curves between the two length extremes, and will therefore have an extended flat region between the increase at low pressure for the largest scale, and the increase at high pressure for the shortest scale. This is plotted in Fig. 15 (V_{bd} versus pressure) for argon for different minimum gaps, assuming a maximum size scale of 500 μm. This approach describes very well our He and Ar data, since for both those gases the effect of the PCB length scales were clearly visible. For nitrogen, one would have to work below 500 Pa (5 mbar) to see any effect of the PCB, so we end up with nearly standard Paschen curves in N_2.

A flattening of the Paschen curves below the predicted upturn pressure was observed by Osmokrovic et al.[13] for Rogowski-type electrodes (but not cylindrical electrodes) for gaps from 0.1 to 0.5 mm with 8-mm-diam electrodes. Rogowski electrodes are rounded and thus allow length scales ranging from the gap up to much longer distances. A similar explanation was proposed (that breakdown occurs at different gaps for different pressures).

When operating at a pressure of one atmosphere, the situation is simpler with respect to the different length

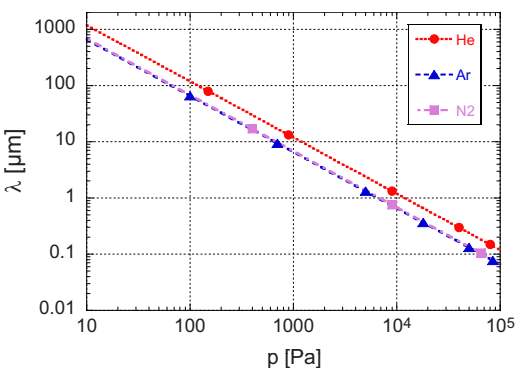

Fig. 12 Calculated main free path length λ versus pressure P for different gases: helium, argon, and nitrogen.

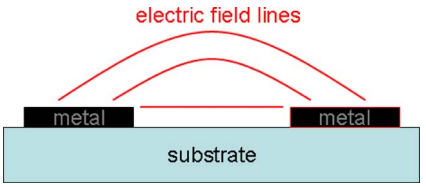

Fig. 13 Illustration of three different length scales for the electric field in a planar geometry.

scales present in a planar geometry. Indeed, Paschen curve data taken at one atmosphere in Ref. 4 do not show any evidence of multiple length scales. Figure 16 is a theoretical plot of V_{bd} versus gap size in argon, with the same parameters as in Fig. 1, but plotted for a fixed pressure of 10^5 Pa. At this high pressure, the minimum V_{bd} of the Paschen curve is pushed down to approximately 5 μm. So for gaps larger than 10 μm at one atmosphere, it is the smallest gap that dictates the breakdown voltage. The fact that the geometry is planar is then of no consequence, unlike at reduced pressures.

5 Conclusions

An experimental study is presented of the breakdown voltage of microfabricated 8-μm-thick aluminum electrodes with gaps ranging from 10 to 500 μm. The pressure is varied from 500 to 8.10^4 Pa (5 to 800 mbar) in helium, argon, and nitrogen atmospheres. The breakdown voltage is plotted as a function of the Paschen reduced variable $P_{red} = P \cdot d$. For higher values of pressure or gap (high P_{red}), classical Paschen scaling is observed for all three gases. For lower values of P_{red}, however, significant deviations are seen, particularly at low pressures. These differences cannot be attributed to field emission, since the effect occurs at gaps of several hundred microns.

At low values of P_{red}, the mean free path becomes of the order of the gap spacing, which explains the slightly higher than expected breakdown voltages seen in this range. The many length scales effectively present in our planar geometry (on-chip and even off-chip) that lead to the superposition of several Paschen curves explain the difficulty in using the Paschen theory to fit over the full $P \cdot d$ range. Taking the many length scales into account allows for explaining the three regimes in the V_{bd} versus pressure curves for a fixed electrode gap: at low pressures the curve is given by the Paschen theory computed using the largest spacing in the system, at intermediate pressures V_{bd} is constant and corresponds to the minimum in the Paschen curve for that gas and electrode material, and at higher pressures the curve is the standard Paschen curve using the smallest gap in the system.

To ignite a dc plasma on-chip, V_{bd} must be exceeded. This voltage is gas dependent, for instance, significantly lower in He than in N_2. The lowest V_{bd} values in He are obtained for electrodes with serrated patterns and range from 170 to 210 V. While a smaller electrode gap does increase the maximum electric field, at low pressures this is not particularly relevant in view of the Paschen theory, and especially in view of the many length scales present in the planar geometry. For igniting plasmas at low pressures, comparable ignition voltages are found for a wide range of gap sizes, and the electrode spacing can then be driven by other considerations, such as fabrication technology or de-

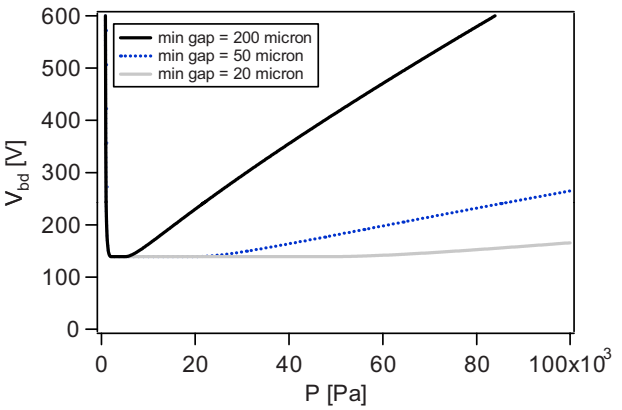

Fig. 15 Computed V_{bd} versus pressure plots taking multiple length scales into account, i.e., the minimum envelope of the curves in Fig. 14. The three curves correspond to three minimum gaps (20, 50, and 200 μm) for a maximum length scale of 500 μm.

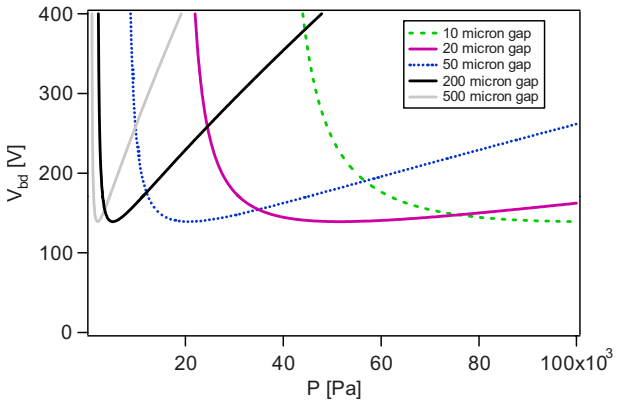

Fig. 14 Theoretical V_{bd} versus pressure for five gaps in argon. The larger the gap, the smaller the pressure, where V_{bd} is minimum. If all the length scales are present, the measured Paschen curve will be the minimum envelope of all the curves.

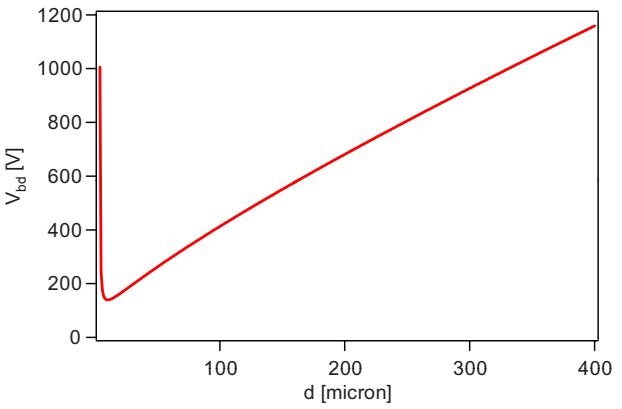

Fig. 16 Paschen curve for argon at a pressure of 1 atmosphere. Since the minimum in V_{bd} occurs for a gap of 5 μm, the breakdown voltage is given directly by the Paschen curve computed with the minimum gap as long as the gap is larger than 5 μm.

vice capacitance. If breakdown is to be avoided, one must then note that lower pressures lead to lower breakdown voltages: the minimum safe operation voltage for a given gap decreases linearly with pressure from the value at one atmosphere over a large pressure range.

At pressures below one atmosphere, care must be taken when applying the Paschen formula to gaps in the micron range. For operation at one atmosphere, standard Paschen behavior is observed for gaps larger than 10 μm.

References

1. R. S. Dhariwal, J. M. Torres, and M. P. Y. Desmulliez, "Electric field breakdown at micrometre separations in air and nitrogen at atmospheric pressure," *IEE Proc.: Sci., Meas. Technol.* **147**(5), 261–265 (2000).
2. J. M. Torres and R. S. Dhariwal, "Electric field breakdown at micrometre separations," *Nanotechnology* **10**, 102–107 (1999).
3. P. G. Slade and E. D. Taylor, "Electrical breakdown in atmospheric air between closely spaced (0.2 μm–40 μm) electrical contacts," *IEEE Trans. Compon. Packag. Technol.* **25**(3), 390–396 (2002).
4. A. Wallash and L. Levit, "Electrical breakdown and ESD phenomena for devices with nanometer-to-micron gaps," *Proc. SPIE* **4980**, 87–96 (2003).
5. C. H. Chen, J. A. Yeh, and P. J. Wang, "Electrical breakdown phenomena for devices with micron separations," *J. Micromech. Microeng.* **16**, 1366–1373 (2006).
6. F. W. Strong, J. L. Skinner, and N. C. Tien, "Electrical discharge across micrometer-scale gaps for planar MEMS structures in air at atmospheric pressure," *J. Micromech. Microeng.* **18**, 075025 (2008).
7. M. J. Schönhuber, "Breakdown of gases below Paschen minimum: basic design data of high-voltage equipment," *IEEE Trans. Power Appar. Syst.*, **PAS-88**, 100 (Feb. 1969).
8. F. Paschen, "Über die zum funkenübergang in luft, wasserstoff und kohlensäure bei verschiedenen drucken erforderliche potentialdifferenz," *Ann. Phys. Chem.* **273**(5), 69–96 (1889).
9. J. Townsend, *Electricity in Gases*, Oxford University Press, New York (1915).
10. H. Jacobs and A. P. LaRocque, "Minimum sparking potentials of barium, magnesium, and aluminum in argon," *J. Appl. Phys.* **18**, 199–203 (1947).
11. L. Baars-Hibbe, P. Sichler, C. Schrader, N. Lucas, K.-H. Gericke, and S. Büttgenbach, "High frequency glow discharges at atmospheric pressure with micro-structured electrode arrays," *J. Phys. D: Appl. Phys.* **38**, 510–517 (2005).
12. N. St. J. Braithwaite, "Introduction to gas discharges," *Plasma Sources Sci. Technol.* **9**, 517–527 (2000).
13. P. Osmokrovic, M. Vujisic, K. Stankovic, A. Vasic, and B. Loncar, "Mechanism of electrical breakdown of gases for pressures from 10^{-9} to 1 bar and inter-electrode gaps from 0.1 to 0.5 mm," *Plasma Sources Sci. Technol.* **16**, 643–655 (2007).
14. L. Baars-Hibbe, P. Sichler, C. Schrader, C. Gessner, K. H. Gericke, and S. Büttgenbach, "Micro-structured electrode arrays: atmospheric pressure plasma processes and applications," *Surf. Coat. Technol.* **174–175**, 519–523 (2003).
15. C. Schrader, L. Baars-Hibbe, K. H. Gericke, E. M. van Veldhuizen, N. Lucas, P. Sichler, and S. Büttgenbach, "Micro-structured electrode arrays: glow discharges in Ar and N_2 at atmospheric pressure using a variable radio frequency generator," *Vacuum* **80**, 1144–1148 (2006).
16. T. Ono, D. Y. Sim, and M. Esashi, "Micro-discharge and electric breakdown in a micro-gap," *J. Micromech. Microeng.* **10**, 445–451 (2000).
17. H. Schlemm and D. Roth, "Atmospheric plasma processing with microstructure electrodes and microplanar reactors," *Surf. Coat. Technol.* **142–144**, 272–276 (2001).
18. P. Carazzetti, P. Renaud, and H. R. Shea, "Low-power hermetically sealed on-chip plasma light sources micromachined in glass," *Proc. IEEE Intl. Conf. MEMS 2008*, pp. 818–821 (2008).
19. P. Carazzetti, P. Renaud, and H. R. Shea, "Micromachined chip-scale plasma light source," *Sens. Actuators, A* (in press).
20. M. A. Hassouba, F. F. Elakshar, and A. A. Garamoon, "Measurement of the breakdown potentials for different cathode materials in the Townsend regime," *Fiz. A* **11**(2), 81–90 (2002).
21. H. Jacobs and A. P. LaRocque, "The role of the cathode surface in sparking phenomena," *Phys. Rev.* **74**(2), 163–165 (1948).
22. L. H. Germer, "Electrical breakdown between close electrodes in air," *J. Appl. Phys.* **30**(1), 46–51 (1959).
23. Y. P. Raizer, *Gas Discharge Physics*, Springer, Berlin (1997).

Patrick Carazzetti holds an MSc in materials science from the EPFL in Lausanne, Switzerland (2002), and a PhD from the Institute of Microtechnology of the University of Neuchâtel, Switzerland (2006). From 2006 to 2008, he was a postdoctoral fellow at the Microsystems for Space Technologies Laboratory, EPFL. His research activity focused on the development of low-power chip-scale plasma sources. In May 2008 he joined the PVD Wafer group at Oerlikon Systems, Balzers, Liechtenstein.

Herbert R. Shea holds a PhD (1997) in physics from Harvard University, and a BSc in physics from McGill University (1991). After two years as a postdoctorate at IBM's T.J. Watson Research Center, he joined Lucent Technologies' Bell Laboratories in Murray Hill, New Jersey, where he became the technical manager of the Microsystems Technology group. Since April 2004, he has been an assistant professor at the EPFL in Lausanne, Switzerland, where he founded the Microsystems for Space Technologies Laboratory. Current research topics include micromachined polymer MEMS (artificial muscles), electric micro-propulsion, MEMS sensors for satellite attitude determination, chip-scale plasma sources, and radiation sensitivity of MEMS.